

# Household Fluorescent Lateral Flow Strip Platform for Sensitive and Quantitative Prognosis of Heart Failure Using Dual-Color Upconversion Nanoparticles

MinLi You,<sup>†,‡</sup> Min Lin,<sup>\*,†,‡,§</sup> Yan Gong,<sup>†,‡,§</sup> Shurui Wang,<sup>†,‡</sup> Ang Li,<sup>||</sup> Lingyu Ji,<sup>⊥</sup> Haoxiang Zhao,<sup>†,‡</sup> Kai Ling,<sup>‡,#</sup> Ting Wen,<sup>§</sup> Yuan Huang,<sup>∇</sup> Dengfeng Gao,<sup>∇</sup> Qiong Ma,<sup>○</sup> Tingzhong Wang,<sup>○</sup> Aiqun Ma,<sup>○</sup> Xiaoling Li,<sup>⊥</sup> and Feng Xu<sup>\*,†,‡,§</sup>

<sup>†</sup>The Key Laboratory of Biomedical Information Engineering of Ministry of Education, School of Life Science and Technology, <sup>‡</sup>Bioinspired Engineering and Biomechanics Center (BEBC), <sup>||</sup>The Key Laboratory of Shaanxi Province for Craniofacial Precision Medicine Research, College of Stomatology, <sup>⊥</sup>School of Mechanical Engineering, and <sup>#</sup>School of Aerospace, Xi'an Jiaotong University, Xi'an 710049, P. R. China

<sup>§</sup>Xi'an Diandi Biotech Company, Xi'an 710049, P. R. China

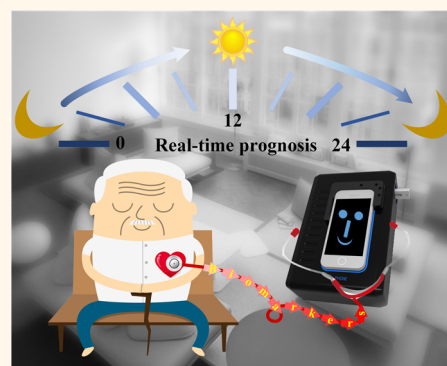
<sup>∇</sup>Department of Cardiology, Second Affiliated Hospital of Xi'an Jiaotong University, Xi'an 710000, Shaanxi, China

<sup>○</sup>Department of Cardiovascular Medicine, First Affiliated Hospital of Xi'an Jiaotong University, Xi'an 710061, Shaanxi, China

## S Supporting Information

**ABSTRACT:** Heart failure (HF) is the end-stage of cardiovascular diseases, which is associated with a high mortality rate and high readmission rate. Household early diagnosis and real-time prognosis of HF at bedside are of significant importance. Here, we developed a highly sensitive and quantitative household prognosis platform (termed as UC-LFS platform), integrating a smartphone-based reader with multiplexed upconversion fluorescent lateral flow strip (LFS). Dual-color core-shell upconversion nanoparticles (UCNPs) were synthesized as probes for simultaneously quantifying two target antigens associated with HF, *i.e.*, brain natriuretic peptide (BNP) and suppression of tumorigenicity 2 (ST2). With the fluorescent LFS, we achieved the specific detection of BNP and ST2 antigens in spiked samples with detection limits of 5 pg/mL and 1 ng/mL, respectively, both of which are of one order lower than their clinical cutoff. Subsequently, a smartphone-based portable reader and an analysis app were developed, which could rapidly quantify the result and share prognosis results with doctors. To confirm the usage of UC-LFS platform for clinical samples, we detected 38 clinical serum samples using the platform and successfully detected the minimal concentration of 29.92 ng/mL for ST2 and 17.46 pg/mL for BNP in these clinical samples. Comparing the detection results from FDA approved clinical methods, we obtained a good linear correlation, indicating the practical reliability and stability of our developed UC-LFS platform. Therefore, the developed UC-LFS platform is demonstrated to be highly sensitive and specific for sample-to-answer prognosis of HF, which holds great potential for risk assessment and health monitoring of post-treatment patients at home.

**KEYWORDS:** household, heart failure, prognosis, lateral flow strip, smartphone-based reader, upconversion nanoparticle



Heart failure (HF) is the end-stage of cardiovascular diseases, arousing about 35% risk of death in the first year after diagnosis<sup>1</sup> and more than 50% patients readmitted to the hospital within 6 months of discharge.<sup>2</sup> Prognosis of HF at home is of vital importance to prevent adverse cardiac events and decrease readmission rate.<sup>3</sup> Existing prognosis methods for HF in clinics mainly rely on the monitoring of physiological indexes (*e.g.*, electrocardiogram, X-ray examination, ultrasound cardiography) and biochemical

indexes (*e.g.*, electrolyte, myocardial enzyme, specific biomarkers). Although physiological indexes can be obtained noninvasively, the need of professional experts for the analysis limits their application at the point of care (POC). In comparison, monitoring of the biochemical indexes can provide

**Received:** April 10, 2017

**Accepted:** May 8, 2017

**Published:** May 8, 2017

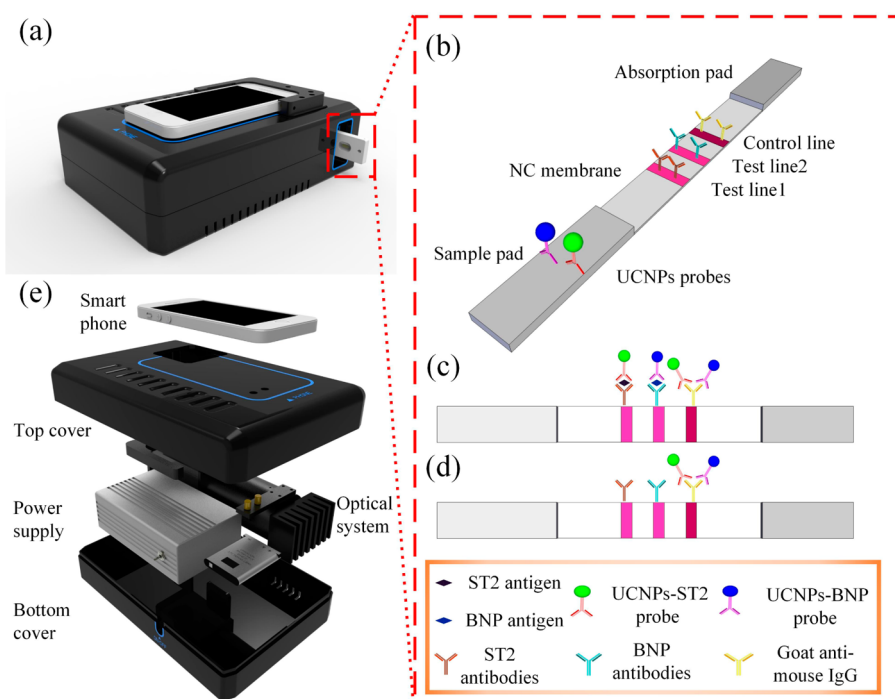


**Figure 1.** Schematic illustration of household fluorescent LFS platform. The multiplexed UC-LFS platform integrating (a) a smartphone-based portable reader and (b) a dual-color UC-NPs-based LFS. (c) When two analytes of BNP and ST2 are present in a sample, the dual-color UC-NPs would be captured in two test lines, respectively. (d) Otherwise, no UC-NPs would be trapped in test lines. Dual-color UC-NPs would be captured in control lines in two cases. (e) The details of smartphone-based reader are displayed in the enlarged view.

accurate biomarker information (*e.g.*, concentration), which is easier for patients to make a judgment of their conditions by comparing with provided reference values. However, monitoring of multiple biomarkers with a high sensitivity is needed to improve the accuracy of HF prognosis. For instance, multiplexed detection of ST2 and BNP (detection limit of  $\sim$ pg/mL level) provides a higher predictive value for HF prognosis than detection of ST2 or BNP independently.<sup>4,5</sup> Besides, the risk for recurrent adverse events of HF patients is assessed in clinics by quantifying specific biomarkers concentrations,<sup>4</sup> which generally relies on sophisticated equipment (*e.g.*, automatic biochemical analyzer), hindering its application at home. Therefore, a multiplexed household platform capable of sensitive and quantitative prognosis of HF is urgently needed.

A paper-based POC test holds great potential to address the above-mentioned issues, with features of being fast, portable, easy-to-use, low cost, and capable of on-site performance.<sup>6</sup> Among various paper based POC tests, lateral flow strip (LFS) is simpler, faster, and cheaper, which is capable of detecting multiple targets and providing results within 20 min with a single-step operation.<sup>6,7</sup> Therefore, LFS is a promising household platform for HF prognosis. Among various LFS technologies, gold nanoparticles (AuNPs)-based LFS has been successfully transformed to an abundance of commercial products due to its low cost and eye-readability of the detection results. Additionally, this technology is also capable of multiple analytes detection *via* design of multiple test lines<sup>8,9</sup> or integration of multiple strips.<sup>10</sup> However, AuNPs-based LFS is associated with limited sensitivity and can only achieve qualitative or semiquantitative detection,<sup>11</sup> thus limiting its application for sensitive and quantitative prognosis of HF.

Recently, various fluorophores have been used to replace AuNPs to improve the sensitivity and quantification capability of LFSs.<sup>12,13</sup> However, popular fluorophores applied in LFSs,

such as fluorescence dye and quantum dots (QDs), are excited by UV light, which involves the issue of strong background signal.<sup>14,15</sup> Besides, fluorescence dye is associated with photobleaching<sup>16</sup> and is unstable under room temperature storage.<sup>17</sup> In comparison, upconversion nanoparticles (UCNPs) emit visible lights upon excitation by NIR light rather than UV light. This unique optical property enables minimized background fluorescence, robust photostability, improved signal-to-noise ratio, and sensitive detection in complex biological samples.<sup>18</sup> Therefore, UCNPs-based LFS has recently attracted increasing attention with widespread applications, including detections of fish infection,<sup>19</sup> antibiotic,<sup>16</sup> parasitic infection,<sup>20</sup> zoonotic pathogens,<sup>21</sup> *etc.* However, the UCNPs-based LFSs generally require bulky and expensive equipment for the excitation of fluorescent signals and readout of the results. Therefore, a small size, cost-effective, and easy-to-use reader is needed for household UCNPs-based LFSs.

Herein, we developed a multiplexed UC-LFS platform for HF prognosis at home, integrating dual-color UCNPs-based LFS and a smartphone-based portable reader. It has the advantages of multiplexed detection, high-sensitivity, and sample-to-answer capability, which is able to directly convert the clinical sample (*e.g.*, serum) to a digital result on a consumer's smartphone. UCNPs with green and blue fluorescence were used for multiplexed detection of BNP and ST2 antigens, respectively, which are associated with the most sensitive marker panels for HF prognosis.<sup>4,5</sup> The green and blue emissions from UCNPs trapped in test lines were measured to quantify the concentrations of BNP and ST2, respectively. Compared with clinical cutoff values, one order higher sensitivity for both BNP and ST2 was achieved. A good specificity of the LFSs was verified by identifying BNP and ST2 from the other four common cardiac markers. To quantitatively

read out the fluorescent LFSs, we also developed a portable reader integrating light source and a smartphone, which is successfully applied in detection of spiked serum with a high recovery level and reproducibility. Subsequently, clinical samples are collected to test, which further confirms the practical reliability and stability of UC-LFS platform. The core-technology in our present work relies on the following aspects: (1) sample-to-answer prognosis for HF based on smartphone reader and LFS; (2) simultaneous detection of two analytes with dual-color UCNP; and (3) stable application to clinical sera. Based on these, we successfully achieved the highly sensitive and multiplex fluorescent LFS detection from clinical sample to digital result on a consumer's smartphone. Overall, the developed UC-LFS platform holds great promise for risk assessment and health monitoring of post-treatment patients at home.

## RESULTS AND DISCUSSION

**Principle of the UC-LFS Platform.** Heart failure is one kind of fatal chronic disease, which requires long-term monitoring of the patients' health. However, there is still a lack of efficient monitoring methods at the POC for HF patients. Herein, we developed a household multiplexed UC-LFS platform for HF prognosis. The platform integrates a dual-color UCNP-based LFS with a smartphone-based portable reader (Figure 1a). To achieve an accurate HF prognosis, two sensitive biomarkers (*i.e.*, ST2 and BNP) were selected. ST2 is a new biomarker listed in 2013 ACCF/AHA guideline for additive risk stratification of patients with HF, while BNP is another independent biomarker capable of improving the predictive value for HF prognosis when combined with ST2.<sup>4,5</sup> The dual-color UCNP probes on a sample pad are responsible for detecting the two biomarkers (Figure 1b). When the sample is added onto the LFS, the target analytes (BNP or ST2 antigens or both) would first specifically bind to UCNP probes forming the UCNP-analyte conjugates. The conjugates would flow through the NC membrane as driven by the capillary force and then be captured by the ST2 and BNP antibodies immobilized in the test lines. The excess UCNP probes without binding analytes would react with the goat antihuman immunoglobulin G (IgG) and be trapped in the control line (Figure 1c). If the analytes are absent in the sample, all UCNP probes would directly flow through the test lines without reaction and be captured on the control line (Figure 1d). After reaction, the fluorescence signal from the LFS could be read by a smartphone-based portable reader, which is designed to be slightly bigger than a palm and composed of a smartphone, top cover, optical system, power supply, and bottom cover (from top to bottom) (Figure 1e). On the left side of the reader, there is a power switch for the device, while the slot for LFS is placed on the right side of the reader. The smartphone is arranged to sit in the holder on the top cover to capture the fluorescence image from the tested LFS. As the main functional part of the reader, the optical system is optimally designed to concentrate the excitation laser, involving a small size laser to produce NIR excitation light and a group of optical lenses to control the inner light route (Figure S1). Comparing the laser power irradiated on LFS with and without the designed device, we found a maximal 3.5 times enhancement of laser power obtained by the designed device (Figure S2).

**Characterization of UCNP.** Detection limit of LFS refers to the lowest concentration of the detected target, whose signal can be distinguished from that of control group. Hence, for a

certain amount of fluorescent nanoparticles captured in test lines, higher fluorescence efficiency of single nanoparticle results in higher detection sensitivity of LFS. Due to the low quantum yield of traditional UCNP, various methods have been proposed to improve its quantum yield, such as optimizing the host materials,<sup>22</sup> coating active shell onto the core UCNP,<sup>23</sup> and using plasmon nanotenna architecture.<sup>24</sup> Here, lanthanides-doped hexagonal-phased NaYF<sub>4</sub> with a shell coating, which has been shown to possess enhanced quantum yield,<sup>25,26</sup> was adopted as the efficient upconversion signal particles. We synthesized hexagonal-phased NaYF<sub>4</sub>:Er,Yb with green fluorescence and NaYF<sub>4</sub>:Tm,Yb with blue fluorescence using the thermal decomposition method. The synthesized hexagonal-phased UCNP were confirmed by the powder X-ray diffraction (XRD) patterns (Figure S3). To decrease the fluorescence quenching effect on UCNP surface, we coated the UCNP core with NaYF<sub>4</sub> shell (Figure 2a–d), resulting in enhanced upconversion fluorescent intensity (the inset graph of Figure 2a–d). To analyze the size distributions of UCNP before and after shell coating, we performed TEM testing and found that the thickness of the shell layer on green and blue UCNP is ~17 nm and ~12 nm, respectively (Figure S4). The measured fluorescence intensities indicate ~8 times emission enhancement for green UCNP and ~3 times emission enhancement for blue UCNP, as reflected by the integral of green emission zone from 500 to 600 nm and blue emission zone from 400 to 500 nm (Figure 2e). To obtain water-soluble and modifiable UCNP, we used PAA to replace the oil acid on the surface of UCNP via a ligand exchange method.<sup>27</sup> The presence of PAA on the surface of UCNP was confirmed by Fourier transform infrared spectroscopy (FTIR), Figure S5. The carboxyl group of PAA was then conjugated with an amino group of McAb under catalysis by EDC and sulfo-NHS. The obtained UCNP-McAb complex dissolved well in water. To verify the successful conjugation of McAb, we measured the dynamic light scattering (DLS) and zeta potential of core-shell UCNP (NaYF<sub>4</sub>:Yb,Tm@ and NaYF<sub>4</sub>:Yb,Er@) UCNP@PAA and UCNP@McAb. We observed that the hydrodynamic size of UCNP increased after McAb conjugation, suggesting the successful conjugation of McAb (Figure 2f). We measured the zeta potential of UCNP after McAb conjugation and found that the zeta potential decreased from -31.16 to -7.96 mV for NaYF<sub>4</sub>:Yb,Er and from -33.68 to -11.7 mV for NaYF<sub>4</sub>:Yb,Tm (Figure 2g). The decrease in zeta potential indicates successful conjugation of McAb as has been demonstrated by literature on antibodies conjugation.<sup>28,29</sup>

### Sensitivity of Single-Color LFSs for BNP and ST2.

Before multiplexed detection, we tested the sensitivity of single-color LFS for BNP and ST2 detection separately. An important element related to LFS detection sensitivity is the quantity of modified antibodies per nanoparticle, which determines the binding efficiency of each particle with target analyte.<sup>30</sup> To optimize this element, we used different concentrations of antibodies (*e.g.*, 12.5, 25, and 50  $\mu\text{g}/\text{mL}$ ) to conjugate with UCNP, and the obtained UCNP probes were utilized to detect a relatively low concentration of target analytes (*i.e.*, 3.5 ng/mL ST2 antigen and 10 pg/mL BNP antigen). Through comparing the fluorescent intensities of test lines, we found that the most sensitive probes are the green UCNP modified with 50  $\mu\text{g}/\text{mL}$  ST2 antibodies and the blue UCNP modified with 25  $\mu\text{g}/\text{mL}$  BNP antibodies (Figure S6). The two optimized probes were applied in the following experiments. Subsequently, standard solutions with different analyte concentration



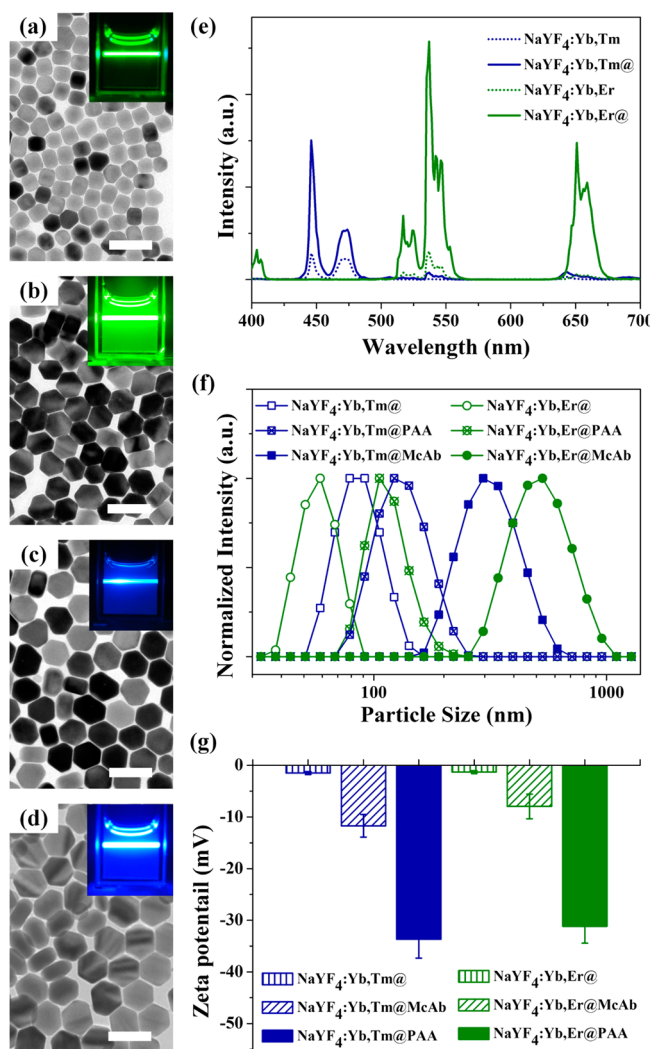


**Figure 2.** Characterization of UCNPs. A  $\text{NaYF}_4$  shell is coated on surface of UCNP cores to enhance the fluorescence intensity. TEM of  $\text{NaYF}_4:\text{Yb,Er}$  (a) before and (b) after  $\text{NaYF}_4$  coating and  $\text{NaYF}_4:\text{Yb,Tm}$  (c) before and (d) after  $\text{NaYF}_4$  coating are performed, and the corresponding fluorescence images are shown as insert graphs. (e) The fluorescence spectra of four UCNPs are displayed, confirming the enhancement of fluorescence emission from shell coating. (f) DLS and (g) zeta potential of core-shell UCNPs ( $\text{UCNPs}@$ ) UCNPs@PAA and UCNPs@McAb are performed to verify the antibodies conjugation. The scale bars represent 100 nm.

were prepared to test the sensitivity of single-color LFS (Figure 3). First, we tested the sensitivity of single-color LFS for BNP detection and found that the fluorescence intensity of the test lines increased with increasing BNP concentration (from 0 to 100 pg/mL). The visible fluorescence signal from test line indicates that the single-color LFS for BNP detection reaches a detection limit of as low as 5 pg/mL (Figure 3a), which was one order lower than that of the clinical cutoff value (100 pg/mL). This was further confirmed by the quantification of the fluorescence intensities of test lines (Figure 3b). Second, we tested the sensitivity of single-color LFS for ST2 detection. We observed that the fluorescence intensity of the test lines increased with increasing ST2 concentration (from 0 to 25 ng/mL). The fluorescence signal remains visible in the test line when the ST2 antigen concentration goes down to as low as 1

ng/mL, suggesting that the detection limit of single-color LFS for ST2 detection reaches 1 ng/mL. The achieved detection limit is one order lower than that of clinical cutoff value (35 ng/mL) for ST2 detection (Figure 3c). This was further confirmed by the quantification of the fluorescence intensities of test lines (Figure 3d).

**Sensitivity of Dual-Color Based Multiplexed LFS.** The dual-color-based multiplexed LFS composed of two test lines (embedded with BNP or ST2 antibodies) and one control line (Figure 4a). To test the sensitivity, we simultaneously tested the BNP and ST2 antigens and recorded the resulted fluorescence images (Figure 4b). The cyan color as observed in the control line comes from the merging of blue and green UCNPs, indicating that the tested dual-color LFSs are valid. We observed that the fluorescence intensities in the test lines increased with increasing concentrations of both BNP and ST2. The strip used to detect 5 pg/mL BNP and 1 ng/mL ST2 antigens shows visible fluorescence on both test lines, indicating that the dual-color LFS possesses multiplexed detection capability and maintains the same high sensitivity as compared with single-color LFS. The quantitative results indicate a good linear relationship between the blue fluorescence intensity of test line 2 and green fluorescence intensity of test line 1 and  $\log[\text{concentration of BNP and ST2 antigens}]$ , respectively (Figure 4c,d). It should be noted that the green fluorescence of test line 2 and blue fluorescence of test line 1 remain at a relatively low level, indicating that the cross-reaction is negligible in the dual-color-based multiplexed LFSs (Figure 4c,d). It is noteworthy that the increase of green fluorescence of test line 2 was caused by the over exposure rather than the nonspecific conjugation of green UCNPs. Therefore, the dual-color-based multiplexed LFS can not only achieve multiplexed detection with a high sensitivity but also possesses the ability to verify the cross-reaction between the target biomarkers.

**Specificity of Dual-Color-Based Multiplexed LFS.** The specificity of the immunoassay is another crucial factor for the detection, which is normally associated with the antibody-antigen binding specificity. Therefore, to evaluate the specificity of dual-color-based multiplexed LFS, four common cardiac markers (*e.g.*, Myo, CTNI, NT-proBNP, CRP) were selected as interfering analytes. The concentrations of four cardiac markers were prepared at 10 times of their clinical cutoff value. The resulted fluorescence images of all the six cardiac markers detection were recorded under the same condition (the inset graphs of Figure 5). Compared to the four interfering cardiac markers, the positive group (simultaneous detection of BNP and ST2) shows a high relative intensity ratio (3.29 for test line 1, 4.03 for test line 2), which is one order higher than the ratio of the four interfering markers (Figure 5). The results indicate that there exists a negligible cross-reaction effect from the other four interfering cardiac markers, even for the homologous metabolites of BNP (*i.e.*, NT-proBNP). These results indicate that the dual-color-based multiplexed LFS could well distinguish target markers from other interfering cardiac markers, thus confirming the good specificity.

**Smartphone-Based Portable Reader.** The readout of the fluorescent LFS generally depends on complicated and expensive readers, which heavily limits its applications in resource-limited areas. To address this, we developed a smartphone-based portable reader for the readout of upconversion fluorescent LFSs (Figure 6a). This reader integrates a portable power, a NIR laser, and a designed optical system. Consumers could use their own smartphone

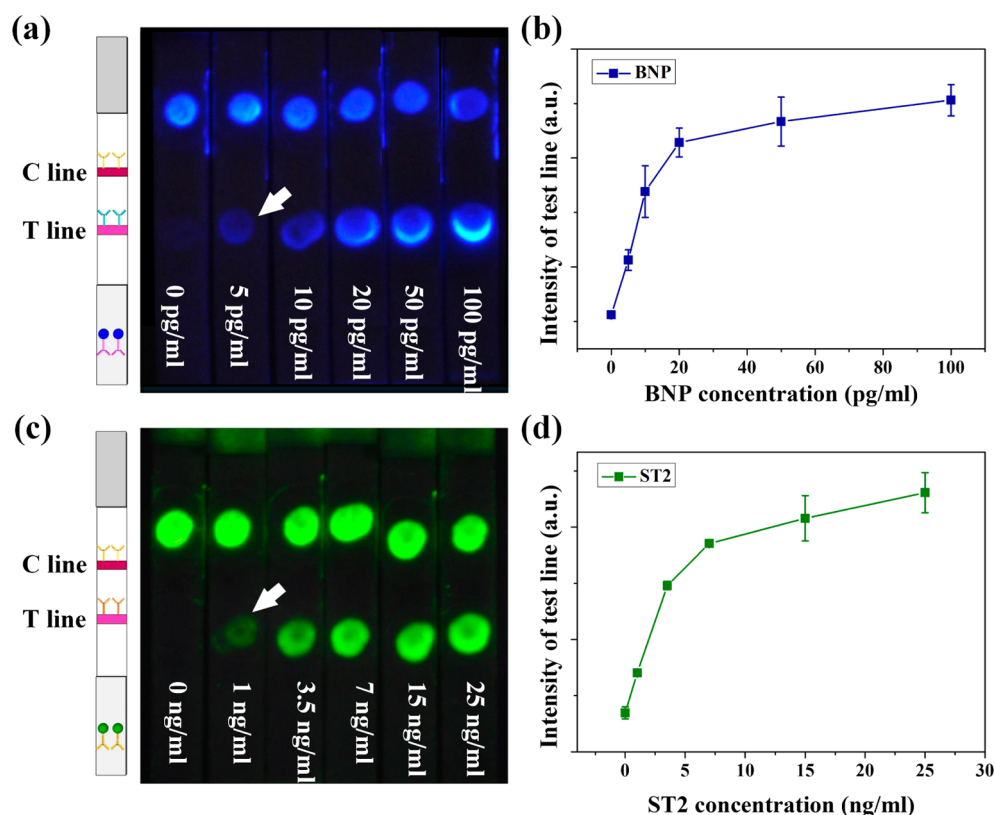


**Figure 3.** Characterization of sensitivity of single-color LFSs. Photographs of single-color LFSs for detecting (a) BNP and (c) ST2 antigens at different concentrations; the insets showing schematic images of single-color LFSs. By quantifying the fluorescence intensities of test lines, the relationships between the fluorescence intensity of test lines and the concentration of (b) BNP and (d) ST2 antigens are obtained.

camera to directly capture the fluorescent images of LFSs through the developed reader. To evaluate the accuracy of the developed reader, we performed results analysis upon the same group of detected LFSs using the developed reader and the traditional method (using Nikon D90 camera to capture fluorescence images and computer to measure the values), respectively. The results show a very good linear correlation, confirming the capability of developed reader to read the fluorescent LFS (Figure 6b,c). Based on the equations shown in Figures 4c,d and 6b,c, we obtained the linear equations between normalized value from phone image and target concentrations (BNP:  $y = 0.598x + 0.182$ , ST2:  $y = 1.374x + 0.915$ , where  $y$  is the normalized value from phone image,  $x$  is the log [target concentration]). To expand the feasibility of the developed reader for various smartphones, we replaced the smartphone holder with a nonslip mat assembled on the top cover (Figure S7). Three smartphones (*i.e.*, Redmi Note, Mi 5, and 360 N 4s) were utilized to read out the same LFS by the reader, and we did not observe significant difference between results obtained from three different smartphone (Figure S8). Furthermore, a smartphone app termed as UC-LFS platform analyzer was also developed to quantify the obtained images (Figure 6d). The main menu of UC-LFS platform analyzer contains three functional buttons of “New capture”, “Import”, and “Share” (Figure 6e). “New capture” and “Import” allow two different ways to obtain images for analysis. “Share” is used to share the analyzed results with the doctors or family members *via* networks. Since the test lines of the strip are manually dropped in the NC membrane, their positions in NC membrane are not consistent so that the signals are hard to autorecognize by the app. Therefore, three manual steps are designed to select the

signal zones of the loaded image, which correspond to “Select blue dot”, “Select green dot”, and “Select reference area”, respectively (Figure 6f). The UC-LFS platform analyzer first calculates the average values of the three selected zones and then normalizes the average values of blue and green dots by dividing by that of the reference area. According to the linear equations between normalized value from phone image and log [target concentration], the concentration of each analyte could be calculated and shown on the smartphone screen, where the analyzed results are displayed in red color, while the clinical cutoff is in green color (Figure 6g).

**Detection of Spiked Serum.** To evaluate the usage of the UC-LFS platform for real samples, a range of different concentrations of spiked sera (*i.e.*, 0, 50, 100, 200, 500, 1000 pg/mL BNP antigens and 0, 10, 35, 70, 150, 250 ng/mL ST2 antigens) were prepared. Since the detection limit of UC-LFS platform is one order lower than the clinical cutoff value, the sample volume required for detection can be reduced. Therefore, 10  $\mu$ L of spiked serum was first diluted 10 times with HSLF buffer and then applied in the following tests. The LFSs after detection were read by the developed reader, and the detected concentrations were compared with the added concentrations (Table 1). We found that the UC-LFS platform had a high recovery level and low variability in low analyte concentrations (below 500 pg/mL for BNP and 150 ng/mL for ST2). However, the variability rose to 40% in high analyte concentration, which significantly reduces the detection accuracy. There may be two possible reasons: one is the exponential relationship between fluorescence intensity of test line and analyte concentration, where slight change in fluorescence intensity results in severe variation of analyte

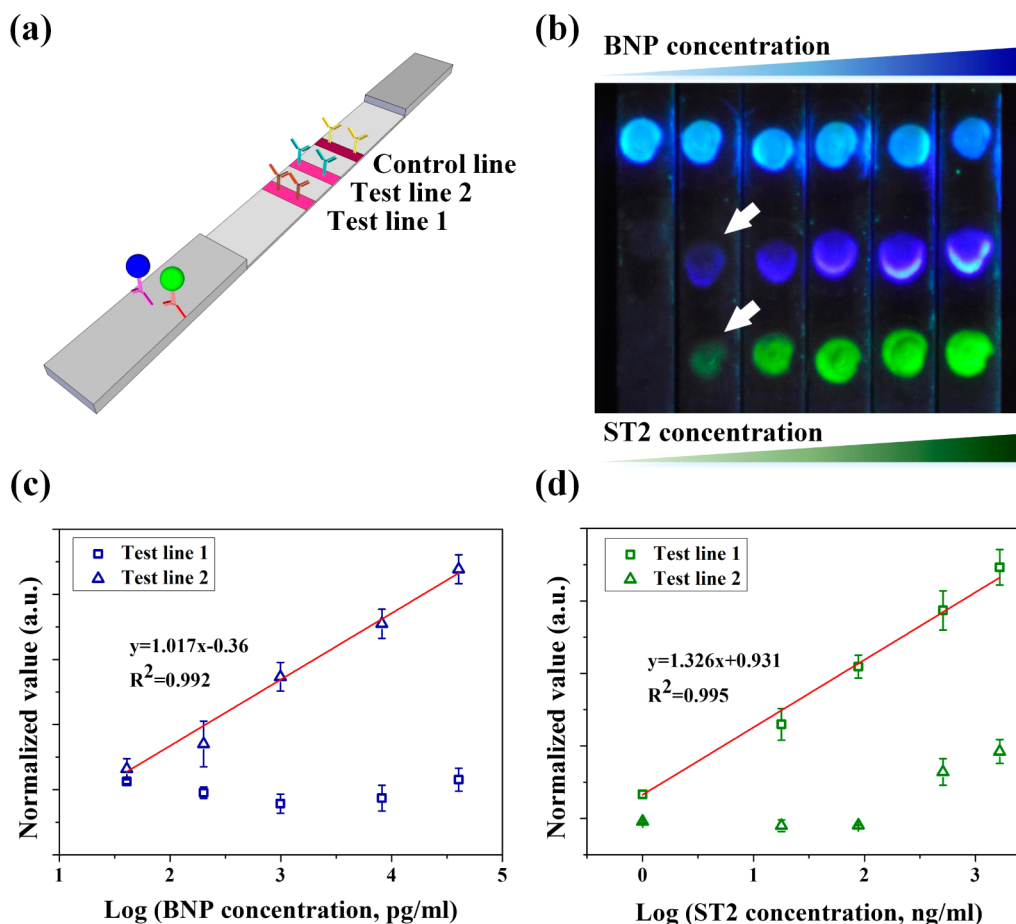


Figure 4. Characterization of sensitivity of dual-color-based multiplexed LFS. (a) Schematic image and (b) photograph of dual-color-based multiplexed LFS for simultaneously detecting BNP and ST2 antigens. By quantifying the fluorescence intensities of test lines through blue and green channels, the relationships between normalized values of fluorescence intensities and log concentrations of (c) BNP and (d) ST2 antigens are obtained.

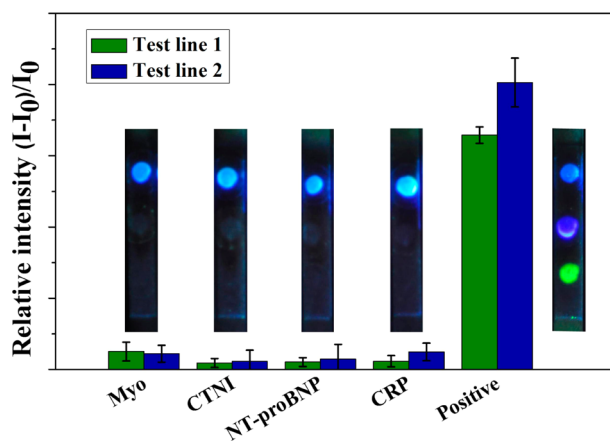
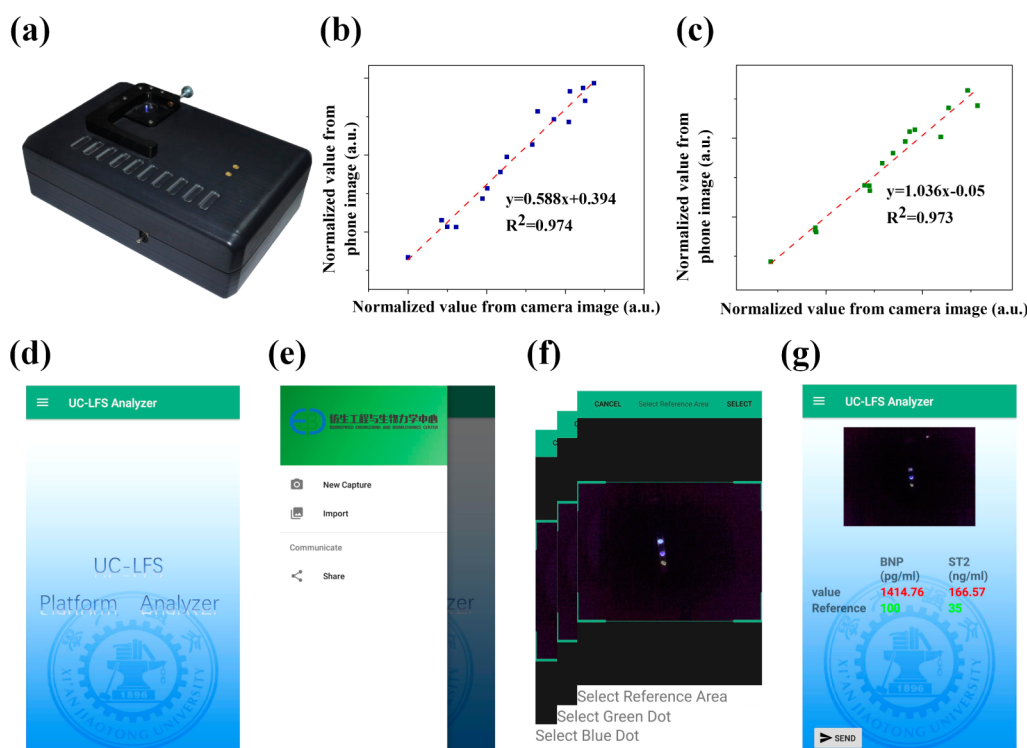


Figure 5. Specificity evaluation of dual-color-based multiplexed LFS for different cardiac biomarkers. Four interfering cardiac biomarkers of Myo, CTNI, NT-proBNP, and CRP, respectively, with 1  $\mu\text{g/mL}$ , 0.6 ng/mL, 4 ng/mL, and 100  $\mu\text{g/mL}$  (all concentrations represent 10 times of their clinical cutoff values) are selected to verify the specificity of dual-color-based LFS. The concentrations of ST2 and BNP in positive group are 25 ng/mL and 100 pg/mL.  $I$  represents the fluorescence intensities of test lines, and  $I_0$  represents the background fluorescence intensity.

concentration when analyte concentration is at a relatively high level; the other is manual selection of signal zones, which brings a subject-to-subject difference. For the HF prognosis, high analyte concentrations of  $>500$  pg/mL BNP or  $>150$  ng/mL ST2 belong to the most dangerous classification and need to be sent to the hospital in minutes.<sup>31,32</sup> From this point of view, the inaccuracy of high analyte concentration (1000–2000 pg/mL for BNP antigen, 150–270 ng/mL for ST2 antigen) does not make a significant effect on the risk classification of HF. Moreover, the subject-to-subject difference could be potentially avoided by changing the fabrication manner of the test line from manually dropping to mechanically drawing and using the smartphone app to directly read the fluorescence signal from a fixed position.

**Detection of Clinical Samples.** To assess the prognosis ability of the developed UC-LFS platform for clinical samples, we measured the concentration of BNP and ST2 in 38 serum samples collected from hospitalized patients with heart insufficiency using the developed UC-LFS platform and FDA approved clinical methods (*i.e.*, chemiluminescent immunoassay performed on Beckman DXI800 Immunoassay System for BNP detection, ELISA kit for ST2 detection) separately. As a result, we successfully detected the minimal concentration of 29.92 ng/mL for ST2 and 17.46 pg/mL for BNP, which are both below their clinical cutoff and show slight variation with those of clinical methods (*e.g.*, 30 ng/mL for ST2 and 19 pg/





**Figure 6.** Smartphone-based portable reader. (a) Image of the smartphone-based portable reader. Linear correlation between readout results from portable reader and traditional method for (b) BNP and (c) ST2 detection. Screenshots from the UC-LFS platform analyzer app for (d) start interface, (e) main menu, (f) signal selection, and (g) analysis results. Permission from the authorized agent was obtained for the logos in (d), (e), and (g).

**Table 1.** Recovery Levels of UC-LFS Platform for Target Analytes in Spiked Serum

analytes	added concentration	detected concentration	R (%)
BNP (pg/mL)	1000	1493.81 ± 497.83	149.4 ± 49.78
	500	500 ± 84.4	100 ± 16.88
	200	202.16 ± 29.78	101.1 ± 14.89
	100	100.45 ± 9.83	100.5 ± 9.83
	50	47.88 ± 3.63	95.8 ± 7.26
ST2 (ng/mL)	250	262.72 ± 107.69	105.1 ± 43.08
	150	148.77 ± 13.35	99.2 ± 8.9
	70	75.94 ± 2.61	108.5 ± 3.73
	35	39.72 ± 1.52	113.5 ± 4.34
	10	8.14 ± 0.92	81.4 ± 9.2

mL for BNP). We then adopted Passing–Boblok regression and Spearman’s rank correlation coefficient to analyze the linear dependence between the two methods. As a consequence, the regression equation and Spearman’s coefficient of rank correlation of BNP detection between clinical chemiluminescent immunoassay and UC-LFS platform were  $y = 1.17$  (95% CI, 1.09–1.25)  $x - 21.49$  (95% CI, -1.29 to -37.65) and 0.98 (95% CI, 0.94–0.991;  $p < 0.0001$ ), respectively (Figure 7a). The slope of regression equation is smaller than 1.2, and the Spearman’s coefficient is close to 1, indicating a good linear relation between the two methods for BNP detection. As for ST2 detection, the regression equation and Spearman’s coefficient of rank correlation between ELISA and UC-LFS platform were  $y = 0.62$  (95% CI, 0.49 to 0.77)  $x + 20.28$  (95% CI, 10.95–28.56) and 0.887 (0.767–0.945;  $p < 0.005$ ), respectively (Figure 7b). The regression equation slopes ranging in 95% CI are larger than 0.49, indicating that the

two methods for ST2 detection possess weak linear correlation. The weak linear correlation in ST2 detection could be attributed to the following reasons:<sup>33</sup> (1) the affinity variance of antibodies from different companies (antibody pair used in ST2 ELISA kit is from Critical Diagnostics and that in LFS assay is from R&D system); (2) the different standards of valuing protein mass when capturing the same molar quantity of proteins; and (3) the effect of different reagents and buffers used in the two methods. However, the weak linear correlation between different detection methods does not represent a poor prognosis capacity of any method. For example, it has been reported in literature that although different detection methods display a weak linear correlation, all the methods possess a good prognosis result for HF patients.<sup>34</sup> Overall, the UC-LFS platform holds great potential for evaluation of family health care and achieving long-distance medicine.

## CONCLUSION

In conclusion, we developed a multiplexed UC-LFS platform integrating dual-color UCNPs-based LFSs and a smartphone-based portable reader for HF prognosis at home. Two kinds of core–shell UCNPs with enhanced green and blue fluorescence were successfully synthesized. Utilizing these two UCNPs, a multiplexed LFS was fabricated for quantitative detection of BNP and ST2 antigens with high sensitivity and specificity. Herein, the two color UCNPs not only allow dual-target detection but also confirm the negligible cross-reaction between the two target biomarkers. The high sensitivity with a detection limit of one order lower than the clinical cutoff values decreases the requirement for patient’s sample. In this case, only a minimum volume of 10  $\mu$ L of serum is needed for each detection. A good specificity of the LFSs was verified by using

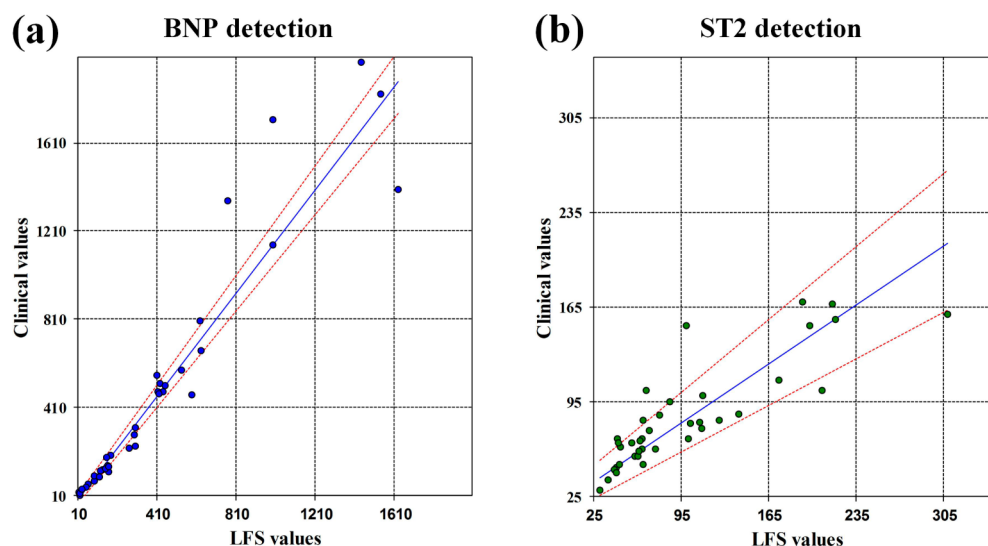


**Figure 7.** Passing–Bablok regression plots between the results obtained from clinical methods and our UC-LFS platform for (a) BNP and (b) ST2 detection in clinical samples. In each figure, the solid blue line represents the linear regression plot, and the two red dash lines show the 95% CI range. The obtained regression equations for BNP and ST2 detection are  $y = 1.17$  (95% CI, 1.09–1.25)  $x - 21.49$  (95% CI, -1.29 to -37.65) and  $y = 0.62$  (95% CI, 0.49–0.77)  $x + 20.28$  (95% CI, 10.95–28.56), respectively.

four interfering cardiac markers. To make the platform for home use, a smartphone-based portable reader and an analysis app were developed to read and analyze the tested dual-color fluorescent LFS, which enable patients to conduct long-distance prognosis with doctors. At last, clinical samples were collected to test in the UC-LFS platform, where the resulting good linear correction with FDA approved clinical methods promises the practical reliability and stability.

LFS test offers many advantages such as simplicity, rapidness, and low cost, while suffers from low accuracy and inability to quantify results. Although an abundance of studies (e.g., fluorescent LFS,<sup>35</sup> dual-AuNP-based LFS,<sup>36</sup> multilayer LFS<sup>37</sup>) have been devoted to addressing these problems, it is still challenging to achieve sensitive, multiplex, and sample-to-answer detection. Moreover, few of these methods have been validated by the detection of clinical samples. Herein, our developed UC-LFS platform not only achieves multiplex sample-to-answer prognosis for HF but also is capable of detecting clinical sera with high sensitivity and stability. Therefore, we envision that the highly sensitive and multiplex UC-LFS platform holds great promise for HF prognosis at home.

## MATERIALS AND METHODS

**Materials.**  $\text{YCl}_3 \cdot 6\text{H}_2\text{O}$ ,  $\text{YbCl}_3 \cdot 6\text{H}_2\text{O}$ ,  $\text{ErCl}_3 \cdot 6\text{H}_2\text{O}$ ,  $\text{TmCl}_3 \cdot 6\text{H}_2\text{O}$ , ammonium fluoride ( $\text{NH}_4\text{F}$ ), poly(acrylic acid) (PAA,  $M_w = 1800$ ), EDC were purchased from Sigma-Aldrich. 1-Octadecene (90%) and oleic acid (90%) were obtained from Alfa Aesar. Methanol, cyclohexane, ethanol, diethylene glycol, sodium hydroxide (NaOH), and 2-(*N*-morpholino)ethanesulfonic acid (MES) were obtained from Tianjinzhiyuan Chemical Reagen Co., Ltd. Sulfo-NHS was purchased from Shanghai Gongjia Chemical Reagen Co., Ltd. All reagents were of analytical grade and used without any purification. Immersing pad (1.9 cm  $\times$  30 cm), nitrocellulose membrane (2.0 cm  $\times$  30 cm), plastic adhesive backing pad, and absorbent pad were obtained from Shanghai Jiening Biotech Co., Ltd. Goat antimouse IgG was obtained from Guangzhou Green Biotechnology Co., Ltd. ST2 antigen and ST2 antibodies were purchased from R&D Systems. BNP antigen and BNP antibodies were purchased from Abcam. NT-proBNP, PCT, CTNI, and Myo antigens were purchased from Fapon Biotech Co., Ltd. The serum samples of patients with III or IV heart function classification

were obtained from Department of Cardiovascular Medicine, Second Affiliated Hospital of Xi'an Jiaotong University School of Medicine. The participants have given written informed consent for scientific research. The Aleric Triage BNP test is performed on Beckman DXI800 Immunoassay System, and Presage ST2 (human) ELISA kits were purchased from Critical Diagnostics.

**Synthesis of Core and Core–Shell UCNPs.** The UCNPs were synthesized following our previous protocol.<sup>38–40</sup> In a typical synthesis of 30 nm-sized  $\beta\text{-NaYF}_4\text{:Er,Yb}$ ,  $\text{YCl}_3 \cdot 6\text{H}_2\text{O}$  (242.69 mg, 0.8 mmol),  $\text{YbCl}_3 \cdot 6\text{H}_2\text{O}$  (69.75 mg, 0.18 mmol), and  $\text{ErCl}_3 \cdot 6\text{H}_2\text{O}$  (7.64 mg, 0.02 mmol) in 2 mL deionized water were added to a 100 mL flask containing 7.5 mL of oleic acid and 15 mL of 1-octadecene. The solution was stirred at room temperature for 0.5 h. Then the mixture was heated to 120 °C for 1 h until no bubbles floating on the liquid could be observed and 156 °C for another 1.5 h to get rid of water under argon atmosphere. The system was then cooled down to room temperature. Subsequently, 10 mL of methanol solution containing  $\text{NH}_4\text{F}$  (148.15 mg, 4 mmol) and NaOH (100 mg, 2.5 mmol) was added into the solution and was then stirred at room temperature for 2 h. The system was then allowed to remove the protection of the argon atmosphere. Then, the system was heated to 120 °C for 1 h. After evaporating the methanol, the solution was heated to 280 °C and maintained for 1.5 h, then cooled down to room temperature. The resulting product was washed with ethanol and cyclohexane for three times and was finally dissolved in cyclohexane. To synthesize  $\text{NaYF}_4\text{:Er,Yb}@NaYF_4$ , the same process was carried out with the amounts of precursors changed as follows:  $\text{YCl}_3 \cdot 6\text{H}_2\text{O}$  (151.68 mg, 0.5 mmol), and the  $\text{NaYF}_4\text{:Er,Yb}$  solution was added into system before addition of methanol solution of  $\text{NH}_4\text{F}$  and NaOH. The synthesis of  $\beta\text{-NaYF}_4\text{:Tm,Yb}$  and  $\beta\text{-NaYF}_4\text{:Tm,Yb}@NaYF_4$  was the same as the above protocol except that the precursors were changed to  $\text{YCl}_3 \cdot 6\text{H}_2\text{O}$  (453.22 mg, 1.494 mmol),  $\text{YbCl}_3 \cdot 6\text{H}_2\text{O}$  (193.75 mg, 0.5 mmol), and  $\text{TmCl}_3 \cdot 6\text{H}_2\text{O}$  (2.3 mg, 0.006 mmol).

**Surface Modification of UCNPs.** To make UCNPs water soluble, a ligand exchange method was used for surface modification of UCNPs. To this end, PAA (150 mg) and diethylene glycol (15 mL) were added into a 50 mL three-necked round-bottomed flask with a stirrer bar. Argon atmosphere was then infused into the system at room temperature. After heating to 110 °C, the chloroform solution of UCNPs was dropped into the system and kept for 1.5 h at 110 °C. After evaporating chloroform, the reaction system was heated to 160 °C for another 1.5 h until the solution became clear. The solution was



then centrifuged at 10,000 rpm for 10 min. After washing 3 times with ethanol and deionized water, the water-soluble particles were obtained.

**Conjugation of Antibodies to UCNPs.** The conjugation of UCNPs and antibodies was realized through (EDC/sulfo-NHS)-mediated amination reaction. Typically, 30  $\mu\text{L}$  of 30 mM EDC and 30  $\mu\text{L}$  of 30 mM sulfo-NHS were first added into redispersed 1 mL of UCNPs MES solution. After 30 min incubation, the activated product was washed for three times with MES buffer and then redispersed in 5 mL of MES buffer. Different amounts of antibodies (12.5  $\mu\text{g}$ , 25  $\mu\text{g}$ , 50  $\mu\text{g}$ ) were added into 1 mL of redispersed MES solution. After 2 h incubation, 30  $\mu\text{L}$  of 2 M glycine stop buffer was added. The obtained UCNPs-antibodies complex was washed for three times with storage buffer (50 mM glycine, 0.1%  $\text{NaN}_3$ , 0.03% v/v triton) and was finally dissolved in 1 mL of storage buffer and was kept at 4  $^\circ\text{C}$ .

**Fabrication of Lateral Flow Strips.** The lateral flow strips were prepared following our previous protocol.<sup>41,42</sup> Immersing pad, nitrocellulose membrane and absorbent pad were orderly mounted on a plastic adhesive backing pad with 2 mm overlap between each two adjacent pads. Subsequently, the as-assembled pads were cut into strips with width of 2.5 mm by Matrix<sup>TM</sup> 2360 Programmable Sheer (Kinematic Automation, Sonora, CA, USA). Test and control zones were separately generated by dispensing 0.5  $\mu\text{L}$  of 2 mg/mL goat antimouse IgG and 0.5  $\mu\text{L}$  of 0.2 mg/mL BNP or ST2 antibodies. The obtained nitrocellulose membranes were dried at 37  $^\circ\text{C}$  for 2 h in a vacuum oven.

**Assays with Fabricated Lateral Flow Test Strips.** UCNPs probe solution was formulated by a mixture of 10  $\mu\text{L}$  of UCNPs-antibodies complex stock solution and 1240  $\mu\text{L}$  of HSLF buffer (270 mM NaCl, 100 mM hepes buffer, 0.5% w/v tween 20, 1% w/v BSA). Standard BNP antigen solution (0, 5, 10, 20, 50, 100 pg/mL) and ST2 antigen solution (0, 1, 3.5, 7, 15, 25 ng/mL) were formulated by diluting the antigen stock solution using sterile water. Spiked BNP sera (50, 100, 200, 500, 1000 pg/mL) and ST2 sera (10, 35, 70, 150, 250 ng/mL) were formulated by diluting the antigen stock solution using normal human sera. After mixing standard antigen solution or spiked serum and UCNPs reporter solution, the obtained solution was added onto the sample pad of LFS. After 20 min, the fluorescence results were read under 980 nm NIR laser excitation using Nikon D90 camera or the developed reader. The LFS was judged as valid when the control line presented a cyan color. The LFS was judged as positive when the test line 1 presented a green color or test line 2 presented a blue color. Each test was repeated three times. The gray values of test lines 1 and 2 were measured through green and blue channels, separately. Then, they were normalized *via* dividing by background signal value.

**Characterization.** The morphologies of the UCNPs were characterized by transmission electron microscopy (TEM) using a JEM 2100 instrument at an accelerating voltage of 200 kV. The XRD patterns of UCNPs powder were characterized on an XRD-7000 diffractometer. A Nano-ZS90 Zeta Sizer was used to determine zeta potentials and dynamic light scatter (DLS) of UCNPs. The FTIR spectra of the nanoparticles were obtained using a Nicolet iS50 Fourier transform infrared spectrophotometer (Thermo Electron Co., USA). The upconversion emission spectra were recorded by using a spectrophotometer (QuantaMasterTM40) under external excitation of a 250 mW 980 nm laser diode (RGB Laser systems). Images of fluorescence strip upon 980 nm CW laser (Changchun Liangli Photoelectric Co., Ltd.) excitation were obtained *via* a Nikon D90 digital Single Lens Reflex with Macrolens and an attached IR filter. The optimized shooting conditions are 8 s exposure time and f/4 aperture size. The laser power is measured by a PM100D Hand-held Optical Power and Energy Meter of Thorlabs, and the used excitation NIR laser is a 980 nm CW laser with adjustable power in the range of 0–10 W (Changchun Liangli Photoelectric Co., Ltd.). All the measurements were performed at room temperature.

## ASSOCIATED CONTENT

### Supporting Information

The Supporting Information is available free of charge on the ACS Publications website at DOI: 10.1021/acsnano.7b02466.

Additional experimental procedures and data (PDF)  
Operational procedure video (AVI)

## AUTHOR INFORMATION

### Corresponding Authors

\*E-mail: minlin@mail.xjtu.edu.cn.

\*E-mail: fengxu@mail.xjtu.edu.cn.

### ORCID

Min Lin: 0000-0002-3259-1955

Feng Xu: 0000-0003-4351-0222

### Notes

The authors declare no competing financial interest.

## ACKNOWLEDGMENTS

This research was financially supported by the National Natural Science Foundation of China (11402192), National Instrumentation Program (2013YQ190467), Fundamental Research Funds for the Central Universities (2016qngz03), and the Open Funding Project of Key Laboratory of Space Nutrition and Food Engineering Laboratory (SNFE-KF-15-09).

## REFERENCES

- (1) *Chronic Heart Failure: National Clinical Guideline for Diagnosis and Management in Primary and Secondary Care*; Royal College of Physicians: London, 2010.
- (2) Desai, A. S.; Stevenson, L. W. Rehospitalization for Heart Failure: Predict or Prevent? *Circulation* **2012**, *126*, 501–506.
- (3) Xanthakis, V.; Enserro, D. M.; Larson, M. G.; Wollert, K. C.; Januzzi, J. L.; Levy, D.; Aragam, J.; Benjamin, E. J.; Cheng, S.; Wang, T. J.; Mitchell, G. F.; Vasan, R. S. Prevalence, Neurohormonal Correlates, and Prognosis of Heart Failure Stages in the Community. *JACC: Heart Failure* **2016**, *4*, 808–815.
- (4) Januzzi, J. L.; Mebazaa, A.; Di Somma, S. ST2 and Prognosis in Acutely Decompensated Heart Failure: The International ST2 Consensus Panel. *Am. J. Cardiol.* **2015**, *115*, 26B–31B.
- (5) Friões, F.; Lourenço, P.; Laszczynska, O.; Almeida, P.-B.; Guimarães, J.-T.; Januzzi, J. L.; Azevedo, A.; Bettencourt, P. Prognostic Value of sST2 Added to BNP in Acute Heart Failure with Preserved or Reduced Ejection Fraction. *Clin. Res. Cardiol.* **2015**, *104*, 491–499.
- (6) Hu, J.; Wang, S.; Wang, L.; Li, F.; Pingguan-Murphy, B.; Lu, T. J.; Xu, F. Advances in Paper-Based Point-of-Care Diagnostics. *Biosens. Bioelectron.* **2014**, *54*, 585–597.
- (7) Choi, J. R.; Tang, R.; Wang, S.; Wan Abas, W. A. B.; Pingguan-Murphy, B.; Xu, F. Paper-Based Sample-to-Answer Molecular Diagnostic Platform for Point-of-Care Diagnostics. *Biosens. Bioelectron.* **2015**, *74*, 427–439.
- (8) Rivas, L.; de la Escosura-Muñiz, A.; Serrano, L.; Altet, L.; Francino, O.; Sánchez, A.; Merkoçi, A. Triple Lines Gold Nanoparticle-Based Lateral Flow Assay for Enhanced and Simultaneous Detection of Leishmania DNA and Endogenous Control. *Nano Res.* **2015**, *8*, 3704–3714.
- (9) Song, S.; Liu, N.; Zhao, Z.; Njumbe Ediage, E.; Wu, S.; Sun, C.; De Saeger, S.; Wu, A. Multiplex Lateral Flow Immunoassay for Mycotoxin Determination. *Anal. Chem.* **2014**, *86*, 4995–5001.
- (10) Li, C.-z.; Vandenberg, K.; Prabhulkar, S.; Zhu, X.; Schnepfer, L.; Methee, K.; Rosser, C. J.; Almeida, E. Paper Based Point-of-Care Testing Disc for Multiplex Whole Cell Bacteria Analysis. *Biosens. Bioelectron.* **2011**, *26*, 4342–4348.
- (11) Choi, J. R.; Hu, J.; Feng, S.; Wan Abas, W. A. B.; Pingguan-Murphy, B.; Xu, F. Sensitive Biomolecule Detection in Lateral Flow

- Assay with a Portable Temperature–Humidity Control Device. *Biosens. Bioelectron.* **2016**, *79*, 98–107.
- (12) Qiu, W.; Xu, H.; Takalkar, S.; Gurung, A. S.; Liu, B.; Zheng, Y.; Guo, Z.; Baloda, M.; Baryeh, K.; Liu, G. Carbon Nanotube-Based Lateral Flow Biosensor for Sensitive and Rapid Detection of DNA Sequence. *Biosens. Bioelectron.* **2015**, *64*, 367–372.
- (13) Duan, H.; Chen, X.; Xu, W.; Fu, J.; Xiong, Y.; Wang, A. Quantum-DoT Submicrobead-Based Immunochromatographic Assay for Quantitative and Sensitive Detection of Zearalenone. *Talanta* **2015**, *132*, 126–131.
- (14) Dai, Y.; Ma, P. a.; Cheng, Z.; Kang, X.; Zhang, X.; Hou, Z.; Li, C.; Yang, D.; Zhai, X.; Lin, J. Up-Conversion Cell Imaging and pH-Induced Thermally Controlled Drug Release from  $\text{NaYF}_4:\text{Yb}^{3+}/\text{Er}^{3+}$ @Hydrogel Core–Shell Hybrid Microspheres. *ACS Nano* **2012**, *6*, 3327–3338.
- (15) Haase, M.; Schäfer, H. Upconverting Nanoparticles. *Angew. Chem., Int. Ed.* **2011**, *50*, 5808–5829.
- (16) Liu, C.; Ma, W.; Gao, Z.; Huang, J.; Hou, Y.; Xu, C.; Yang, W.; Gao, M. Upconversion Luminescence Nanoparticles-Based Lateral Flow Immunochromatographic Assay for Cephalexin Detection. *J. Mater. Chem. C* **2014**, *2*, 9637–9642.
- (17) Xu, Y.; Liu, Y.; Wu, Y.; Xia, X.; Liao, Y.; Li, Q. Fluorescent Probe-Based Lateral Flow Assay for Multiplex Nucleic Acid Detection. *Anal. Chem.* **2014**, *86*, 5611–5614.
- (18) Lin, M.; Zhao, Y.; Wang, S.; Liu, M.; Duan, Z.; Chen, Y.; Li, F.; Xu, F.; Lu, T. Recent Advances In Synthesis and Surface Modification of Lanthanide-Doped Upconversion Nanoparticles for Biomedical Applications. *Biotechnol. Adv.* **2012**, *30*, 1551–1561.
- (19) Zhao, P.; Wu, Y.; Zhu, Y.; Yang, X.; Jiang, X.; Xiao, J.; Zhang, Y.; Li, C. Upconversion Fluorescent Strip Sensor for Rapid Determination of *Vibrio Anguillarum*. *Nanoscale* **2014**, *6*, 3804–3809.
- (20) Corstjens, P. L. A. M.; de Dood, C. J.; Priest, J. W.; Tanke, H. J.; Handali, S.; and the Cysticercosis Working Group in, P. Feasibility of a Lateral Flow Test for Neurocysticercosis Using Novel Up-Converting Nanomaterials and a Lightweight Strip Analyzer. *PLoS Neglected Trop. Dis.* **2014**, *8*, e2944.
- (21) Zhang, P.; Liu, X.; Wang, C.; Zhao, Y.; Hua, F.; Li, C.; Yang, R.; Zhou, L. Evaluation of Up-Converting Phosphor Technology-Based Lateral Flow Strips for Rapid Detection of *Bacillus anthracis* Spore, *Brucella* spp., and *Yersinia pestis*. *PLoS One* **2014**, *9*, e105305.
- (22) Heer, S.; Kömpe, K.; Güdel, H. U.; Haase, M. Highly Efficient Multicolour Upconversion Emission in Transparent Colloids of Lanthanide-Doped  $\text{NaYF}_4$  Nanocrystals. *Adv. Mater.* **2004**, *16*, 2102–2105.
- (23) Vetrone, F.; Naccache, R.; Mahalingam, V.; Morgan, C. G.; Capobianco, J. A. Upconverting Nanoparticles: The Active-Core/Active-Shell Approach: A Strategy to Enhance the Upconversion Luminescence in Lanthanide-Doped Nanoparticles. *Adv. Funct. Mater.* **2009**, *19*, 2924–2929.
- (24) Feng, A. L.; You, M. L.; Tian, L.; Singamaneni, S.; Liu, M.; Duan, Z.; Lu, T. J.; Xu, F.; Lin, M. Distance-Dependent Plasmon-Enhanced Fluorescence of Upconversion Nanoparticles using Polyelectrolyte Multilayers as Tunable Spacers. *Sci. Rep.* **2015**, *5*, 7779.
- (25) Lin, M.; Zhao, Y.; Liu, M.; Qiu, M.; Dong, Y.; Duan, Z.; Li, Y. H.; Pingguan-Murphy, B.; Lu, T. J.; Xu, F. Synthesis of Upconversion  $\text{NaYF}_4:\text{Yb}^{3+},\text{Er}^{3+}$  Particles with Enhanced Luminescent Intensity through Control of Morphology and Phase. *J. Mater. Chem. C* **2014**, *2*, 3671–3676.
- (26) Wang, F.; Liu, X. Recent Advances in the Chemistry of Lanthanide-Doped Upconversion Nanocrystals. *Chem. Soc. Rev.* **2009**, *38*, 976–989.
- (27) Liu, C.; Wang, H.; Li, X.; Chen, D. Monodisperse, Size-Tunable and Highly Efficient  $\beta\text{-NaYF}_4:\text{Yb},\text{Er}(\text{TM})$  Up-conversion Luminescent Nanospheres: Controllable Synthesis and Their Surface Modifications. *J. Mater. Chem.* **2009**, *19*, 3546–3553.
- (28) Yen, C.-W.; de Puig, H.; Tam, J. O.; Gomez-Marquez, J.; Bosch, I.; Hamad-Schifferli, K.; Gehrke, L. Multicolored Silver Nanoparticles for Multiplexed Disease Diagnostics: Distinguishing Dengue, Yellow Fever, and Ebola Viruses. *Lab Chip* **2015**, *15*, 1638–1641.
- (29) Xu, H.; Aguilar, Z. P.; Yang, L.; Kuang, M.; Duan, H.; Xiong, Y.; Wei, H.; Wang, A. Antibody Conjugated Magnetic Iron Oxide Nanoparticles for Cancer Cell Separation in Fresh Whole Blood. *Biomaterials* **2011**, *32*, 9758–9765.
- (30) Mosley, G. L.; Nguyen, P.; Wu, B. M.; Kamei, D. T. Development of Quantitative Radioactive Methodologies on Paper to Determine Important Lateral-Flow Immunoassay Parameters. *Lab Chip* **2016**, *16*, 2871–2881.
- (31) Zilinski, J. L.; Shah, R. V.; Gaggin, H. K.; Gantzer, M. L.; Wang, T. J.; Januzzi, J. L., Jr Measurement of Multiple Biomarkers in Advanced Stage Heart Failure Patients Treated with Pulmonary Artery Catheter Guided Therapy. *Crit. Care* **2012**, *16*, R135.
- (32) Valle, R.; Aspromonte, N.; Carbonieri, E.; De Michele, G.; Di Tano, G.; Giovinazzo, P.; Cioè, R.; Di Giacomo, T.; Milani, L.; Noventa, F. BNP-Guided Therapy Optimizes the Timing of Discharge and the Medium Term Risk Stratification in Patients Admitted for Congestive Heart Failure. *Monaldi Arch. Chest Dis.* **2007**, *68*, 154–164.
- (33) Mueller, T.; Zimmermann, M.; Dieplinger, B.; Ankersmit, H. J.; Haltmayer, M. Comparison of Plasma Concentrations of Soluble ST2 Measured by Three Different Commercially Available Assays: The MBL ST2 Assay, the Presage ST2 Assay, and the R&D ST2 Assay. *Clin. Chim. Acta* **2012**, *413*, 1493–1494.
- (34) Dieplinger, B.; Egger, M.; Gegenhuber, A.; Haltmayer, M.; Mueller, T. Analytical and Clinical Evaluation of a Rapid Quantitative Lateral Flow Immunoassay for Measurement of Soluble ST2 in Human Plasma. *Clin. Chim. Acta* **2015**, *451*, 310–315.
- (35) Hu, J.; Zhang, Z.-L.; Wen, C.-Y.; Tang, M.; Wu, L.-L.; Liu, C.; Zhu, L.; Pang, D.-W. Sensitive and Quantitative Detection of C-Reaction Protein Based on Immunofluorescent Nanospheres Coupled with Lateral Flow Test Strip. *Anal. Chem.* **2016**, *88*, 6577–6584.
- (36) Hu, J.; Wang, L.; Li, F.; Han, Y. L.; Lin, M.; Lu, T. J.; Xu, F. Oligonucleotide-Linked Gold Nanoparticle Aggregates for Enhanced Sensitivity in Lateral Flow Assays. *Lab Chip* **2013**, *13*, 4352–4357.
- (37) Choi, J. R.; Yong, K. W.; Tang, R.; Gong, Y.; Wen, T.; Yang, H.; Li, A.; Chia, Y. C.; Pingguan-Murphy, B.; Xu, F. Lateral Flow Assay Based on Paper-Hydrogel Hybrid Material for Sensitive Point-of-Care Detection of Dengue Virus. *Adv. Healthcare Mater.* **2017**, *6*, 2192–2659.
- (38) You, M.; Lin, M.; Wang, S.; Wang, X.; Zhang, G.; Hong, Y.; Dong, Y.; Jin, G.; Xu, F. Three-Dimensional Quick Response Code Based on Inkjet Printing of Upconversion Fluorescent Nanoparticles for Drug Anti-Counterfeiting. *Nanoscale* **2016**, *8*, 10096–10104.
- (39) Ma, Y.; Ji, Y.; You, M.; Wang, S.; Dong, Y.; Jin, G.; Lin, M.; Wang, Q.; Li, A.; Zhang, X.; Xu, F. Labeling and Long-term Tracking of Bone Marrow Mesenchymal Stem Cells *In Vitro* Using  $\text{NaYF}_4:\text{Yb}^{3+},\text{Er}^{3+}$  Upconversion Nanoparticles. *Acta Biomater.* **2016**, *42*, 199–208.
- (40) You, M.; Zhong, J.; Hong, Y.; Duan, Z.; Lin, M.; Xu, F. Inkjet Printing of Upconversion Nanoparticles for Anti-Counterfeit Applications. *Nanoscale* **2015**, *7*, 4423–4431.
- (41) Li, C.; Hou, Z.; Dai, Y.; Yang, D.; Cheng, Z.; Ma, P. a.; Lin, J. A Facile Fabrication of Upconversion Luminescent and Mesoporous Core-Shell Structured  $\beta\text{-NaYF}_4:\text{Yb}^{3+},\text{Er}^{3+}/\text{mSiO}_2$  Nanocomposite Spheres for Anti-Cancer Drug Delivery and Cell Imaging. *Biomater. Sci.* **2013**, *1*, 213–223.
- (42) Choi, J. R.; Hu, J.; Tang, R.; Gong, Y.; Feng, S.; Ren, H.; Wen, T.; Li, X.; Wan Abas, W. A. B.; Pingguan-Murphy, B.; Xu, F. An Integrated Paper-Based Sample-to-Answer Biosensor for Nucleic Acid Testing at the Point of Care. *Lab Chip* **2016**, *16*, 611–621.